

# We are IntechOpen, the world's leading publisher of Open Access books Built by scientists, for scientists

6,900

Open access books available

185,000

International authors and editors

200M

Downloads

Our authors are among the

154

Countries delivered to

TOP 1%

most cited scientists

12.2%

Contributors from top 500 universities



WEB OF SCIENCE™

Selection of our books indexed in the Book Citation Index  
in Web of Science™ Core Collection (BKCI)

Interested in publishing with us?  
Contact [book.department@intechopen.com](mailto:book.department@intechopen.com)

Numbers displayed above are based on latest data collected.  
For more information visit [www.intechopen.com](http://www.intechopen.com)



# Group IV Materials for Low Cost and High Performance Bolometers

Henry H. Radamson<sup>1</sup> and M. Kolahdouz<sup>2</sup>

<sup>1</sup>*School of Information and Communication Technology, KTH  
Royal Institute of Technology, Kista*

<sup>2</sup>*Thin Film Laboratory, Electrical and Computer Engineering Department,  
University of Tehran, Tehran,*

<sup>1</sup>*Sweden*

<sup>2</sup>*Iran*

## 1. Introduction

Infrared (IR) imaging has absorbed a large attention during the last two decades due to its application in both civil and military applications (Per Ericsson et al., 2010; Lapadatu et al., 2010; Sood et al., 2010). Thermal detector is presently revolutionizing the IR technology field and it is expected to expand the market for cameras. These detectors are micro-bolometers and are manufactured through micro-machining of a thermistor material. Since these detectors demand no cryogenic cooling, they provide the opportunity for producing compact, light-weight, and potentially low-cost cameras. The preferred functioning wavelength regions for these detectors are usually 8–12  $\mu\text{m}$  due to the high transparency of the atmosphere in these regions.

Micro-bolometers function through absorption of infrared radiation on a cap layer which warms the bolometer's body and raises the temperature. This temperature change is sensed by a thermistor material integrated in the bolometer, i.e. a material whose resistivity changes with temperature variation. The whole detector body consists of a thin membrane which is thermally isolated and is fastened to the wafer via two thin legs. The legs are connected to a CMOS-based read-out integrated circuit (ROIC). A thin oxide or nitride layer is deposited to ensure the stability of the legs in contact to the ROIC body (see Fig. 1). The whole detector is vacuum encapsulated to reduce effectively the thermal conductance. Signal processing is obtained and multiplexing electronics (CMOS) is integrated within the silicon substrate. All the membranes are in form of pixels which are bonded to a read-out circuit to amplify the generated signal (Kvisterøy et al., 2007; J. Källhammer et al., 2006; F. Niklaus, Kälvesten, & G. Stemme, 2001; F. Niklaus, Vieider, & Jakobsen, 2007).

This chapter will present the benefits and drawbacks of group IV thermistor materials in bolometers. The proposed structures are composed of multi-quantum wells (MQWs) or dots (MQDs), structures of Si(C) (barrier)/SiGe(C) (quantum well layer) and their combination with a Schottky diode.

### 1.1 Thermal detectors

A detector may be simply represented by a thermal capacitance  $C_{th}$  coupled via the thermal conductance  $G_{th}$  to a heat sink at the constant temperature  $T$ . When the detector is exposed to radiation, the temperature variation can be calculated through the heat balance equation. For any thermistor material assuming periodic radiant power, temperature variation is given by (Kruse, McGlauchlin, & McQuistan, 1962; Smith, Jones, & Chasmar, 1968):

$$\Delta T = \frac{\varepsilon \Phi_0}{(G_{th}^2 + \omega^2 C_{th}^2)^{1/2}} \quad (1)$$

where  $\Delta T$  is the optically induced temperature variation due to the incident radiation  $\Phi$  ( $\Phi_0 \exp(i\omega t)$ ) and  $\varepsilon$  is the emissivity of the detector. The usual procedure employed in bolometer detectors to achieve a good IR absorption is depositing a transparent thin metallic film on top of the device. Free electron absorption in metal films guarantees the absorption of about 50% of the incident IR radiation (Liddiard, 1984). In order to further enhance infrared absorbance, a resonant cavity is employed in the detector structure. The resonant cavity involves an absorbing membrane suspended at a distance  $d$  above the cavity reflector metal. The resonant absorbance peaks correspond to the condition for minimum reflectance. The three resonance absorbance peaks are  $\lambda/4$ ,  $3\lambda/4$  and  $5\lambda/4$  in the LWIR spectral band (Schimert et al., 2008).

A more practical design for a bolometer with high performance is to create the cavity within the sensor membrane itself. In this case, a reflective area is (a mirror-like) deposited on the bottom side of the bolometer membrane (Per Ericsson et al., 2010).

The LWIR radiation is within 8-12  $\mu\text{m}$  wavelength region and the maximum absorption is obtained when the total bolometer membrane thickness of suspended membrane including the absorbant cap layer, thermistor material and the reflector layer is  $\sim 2-3 \mu\text{m}$ . This thickness is a rough estimation since the semiconductor thermistor material consists of a multilayer (e.g. Si/SiGe) structure. Thus, the final optimized membrane thickness has to be obtained by optical simulations considering the optical properties of all layers.

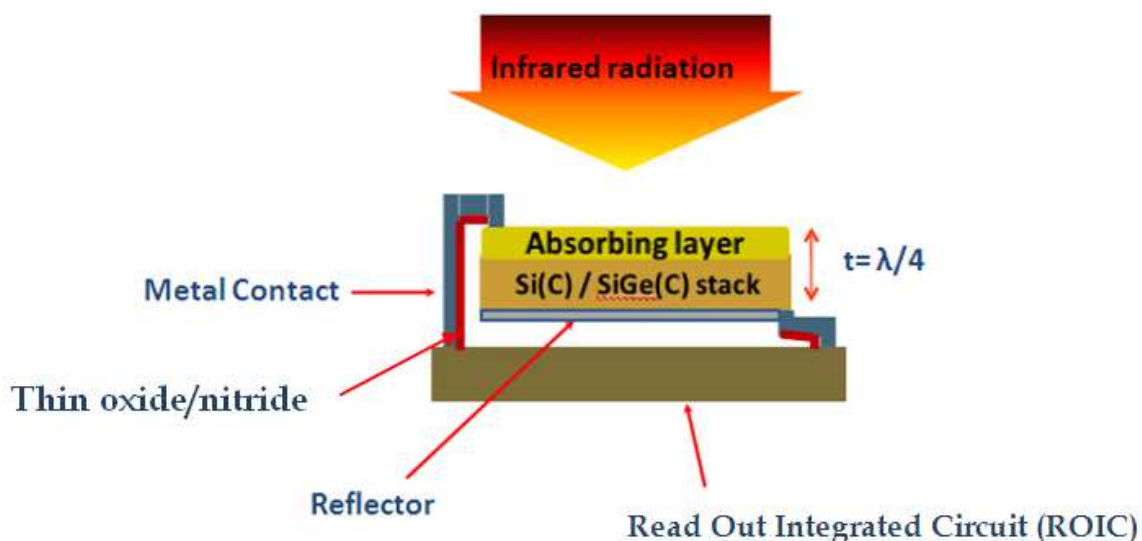


Fig. 1. A schematic cross-section of a bolometer pixel for an optimal absorption.

It is worth mentioning here that for a bolometer, the membrane thickness will affect not only the optical properties, but also the bolometer mass and the electrical resistance. Therefore, it is important to take into account both optical and electrical factors when performing the calculations.

In order to increase the temperature response of the detector, the thermal capacity of the detector ( $C_{th}$ ) and the thermal coupling to its surroundings ( $G_{th}$ ) must be as small as possible. The thermal contacts of the detector with surroundings should be reduced while the interaction with the incident beam must be optimized. In practice, the detectors are vacuum encapsulated to become thermally isolated. The thermal response time ( $\tau_{th}$ ) for such a detector can be written as:

$$\tau_{th} = \frac{C_{th}}{G_{th}} = C_{th}R_{th} \quad (2)$$

The typical response time for a thermal detector is in millisecond range which is longer than that of photon detectors (microsecond range). Eq.1 can then be rewritten as:

$$\Delta T = \frac{\varepsilon\Phi_0 R_{th}}{(1 + \omega^2 \tau_{th}^2)^{1/2}} \quad (3)$$

This means that the detector sensitivity is higher for lower frequency range. The voltage responsivity of the detector is given by the ratio of the output voltage signal ( $V_s$ ) to the input radiation power ( $\Phi_0$ ):

$$R_V = \frac{V_s}{\Phi_0} = \frac{K\Delta T}{\Phi_0} \quad (4)$$

where the generated output voltage is assumed to be linearly proportional to the temperature difference and  $K$  is linearly dependent on the thermistor TCR value. Substituting eq.3 in eq.4 results in the following equation (Liddiard, 1984):

$$R_V = \frac{V_s}{\Phi_0} = \frac{|\alpha| I_s R_b R_L \varepsilon R_{th}}{(R_b + R_L)^2 (1 + \omega^2 \tau_{th}^2)^{1/2}} \quad (5)$$

It can be deduced from the final expression that at low frequencies ( $\omega \ll 1/\tau$ ), the responsivity is proportional to the thermal resistance of the detector ( $R_{th}$ ) and not the thermal capacitance. This is exactly the opposite at high frequencies. As the operating frequency increases beyond the cut-off frequency ( $f = 1/2\pi\tau$ ) the responsivity of the detector rapidly declines. Thus, good responsivity can be achieved by using a high TCR thermistor which is a characteristic of semiconductors rather than metals, and by minimizing  $G_{th}$  through a good thermal isolation of the bolometer.

Thus designing a high quality IR camera is not an easy task and many other parameters and issues e.g. thermistor material choice, costs and feasibility have to be well thought of. Meanwhile a more physical discussion for bolometers should cover the wavelength dependence of the interaction between the optical absorption and the bolometer mass, and

the black body radiance. A more interpretable image of a resistive bolometer can be expressed by the noise equivalent temperature difference (NETD) as follows (Frank Niklaus, Decharat, Jansson, & Göran Stemme, 2008):

$$NETD = \frac{4F^2CV_N(1 + \omega^2\tau_{th}^2)^{1/2}}{\tau_{th}U_{bias}TCR\pi A_{bolo}\frac{\delta}{\delta T_{obj}}\int_{\lambda_1}^{\lambda_2}\phi(\lambda)\varepsilon(\lambda)L(\lambda,T_{obj})d\lambda} [K] \quad (6)$$

where  $\lambda$  is the wavelength and  $T_{obj}$  the object temperature,  $L$  the black body radiance,  $\varepsilon$  the bolometer absorption,  $\phi$  the wavelength dependent transmission of the optical system, TCR the temperature coefficient of resistance,  $U_{bias}$  bias voltage applied to the thermistor,  $\tau$  the thermal time constant of the membrane,  $\omega$  the image modulation frequency,  $V_N$  the RMS noise voltage,  $F$  is the f-number of the optical system, and  $C$  the heat capacity of the membrane.

This expression indicates that the thickness cannot be freely adjusted to obtain the optical  $\lambda/4$  cavity and a larger  $C$  increases the NETD.

## 1.2 Figures of merit for thermistor materials

The figures of merit for a thermistor are temperature coefficient of resistance (TCR) and signal noise level. Today, commonly used thermistor materials such as vanadium oxide ( $VO_x$ ), amorphous, and polycrystalline semiconductors demonstrate moderate noise levels and TCR values around 2%–4% (Lv, Hu, Wu, & Liu, 2007; Moreno, Kosarev, Torres, & Ambrosio, 2007). Recent studies have proposed single crystalline (sc) SiGe as a thermistor material (Di Benedetto, Kolahdouz, Malm, Ostling, & H. H. Radamson, 2009; Vieider et al., 2007; S. Wissmar, H. Radamson, Kolahdouz, & J. Y. Andersson, 2008) demonstrating a high signal-to-noise level. This has been achieved by high epitaxial quality and smooth interfaces between the Si and SiGe layers. The simulations of the fully strained SiGe/Si quantum well structure indicate that the TCR performance can be improved to 6%–8% for 70%–100% Ge in sc-SiGe layers. Although these predicted values for sc-SiGe seem to be outstanding, but so far no experimental data have confirmed the theoretical calculations. One obstacle to overcome is the strain relaxation of the epitaxial SiGe layers which results in surface roughness (Di Benedetto et al., 2009). Since the properties of this thermistor material is improved by increasing the Ge content, producing a high quality SiGe with high Ge content (>35%) is a challenging effort.

## 1.3 Temperature response and sensitivity

The intrinsic part of a bolometer consists of the “thermistor” material. This part responds to temperature variations which result in resistivity changes. The criteria for an ideal thermistor material can be addressed as follows (Schimert et al., 2008): 1) a high temperature coefficient of resistance (TCR); 2) a high signal-to-noise ratio (SNR); 3) a sufficiently low thermal response time constant which leads to a high responsivity; 4) the ability to form a thermally isolated optical cavity from the material; 5) the mature material growth technology that is compatible with integration on a substrate containing the VLSI signal processing functions; and 6) the possibility to manipulate a wide range of bolometer resistance.

Temperature Coefficient of Resistance for a thermistor material is the parameter used to quantify the temperature sensitivity and it is defined as (Di Benedetto et al., 2009):

$$\alpha = \frac{1}{R} \frac{\partial R(T)}{\partial T} [K^{-1}] \quad (7)$$

The resistivity is the exponential function of thermal activation conductance which is expressed by:

$$\rho = \rho_0 \exp\left(\frac{E_a}{kT}\right) \quad (8)$$

where  $\rho$ ,  $\rho_0$ ,  $E_a$  and  $k$  are the resistivity, the measured pre-factor, the activation energy and Boltzmann's constant. In semiconductors,  $\alpha$  can be expressed by the activation energy derived from Arrhenius plot (Schimert et al., 2008):

$$\alpha = -\frac{1}{kT^2} \left[ \frac{3}{2} k_B T + E_f - V \right] \quad (9)$$

The thermistor materials have either positive temperature coefficient of resistance (PTC) or negative temperature coefficient of resistance (NTC). The first group includes materials like metals in which the resistance increases with increasing the temperature; whereas, the latter group are composed of semiconductor materials in which the resistance decreases with increasing the temperature.

For a Si(C)/SiGe(C) MQW structure,  $E_a$  becomes the barrier height  $V$  (see Fig. 2). In order to maximize the TCR of bolometers, high Ge content (or even pure Ge) on Si is required.

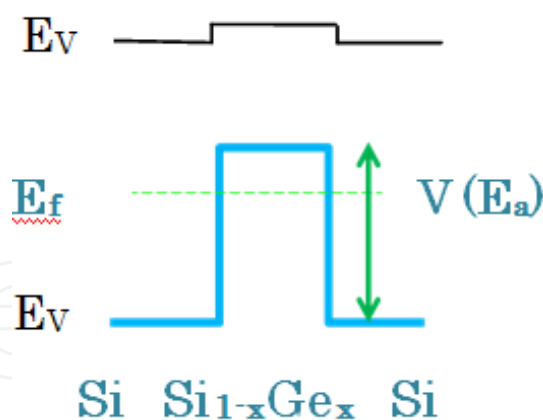


Fig. 2. A schematic drawing of the band diagram of Si/SiGe/Si heterojunctions (type II-alignment).

However, due to lattice mismatch of ~4% between Si and Ge strain relaxation occurs when the thickness of the SiGe layers exceeds a critical value (Bean, Feldman, Fiory, Nakahara, & Robinson, 1984). High quality SiGe quantum wells are grown when the layer thickness is a value within the meta-stable region (see Fig. 3a). Otherwise the strain relaxation for the thin SiGe layers is monitored through interfacial roughness and no dislocations are observed (see Fig. 3b).

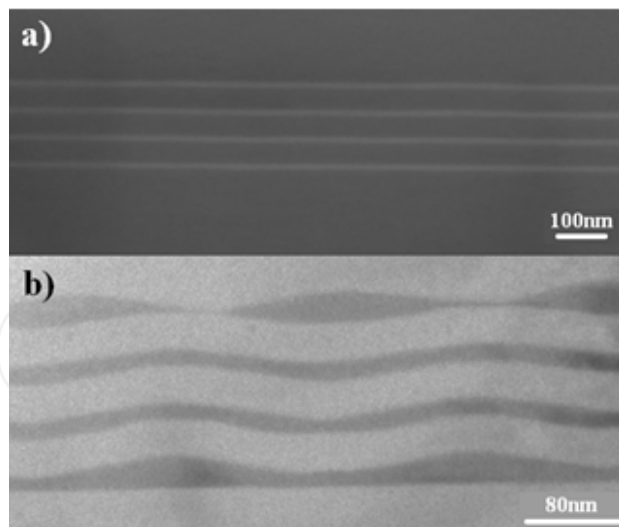


Fig. 3. The cross-sectional HRSEM view of a)  $\text{Si}_{0.72}\text{Ge}_{0.28} / \text{Si}$  and b)  $\text{Si}_{0.68}\text{Ge}_{0.32} / \text{Si}$  stack grown at  $650^\circ\text{C}$ . The dark strips are SiGe layers.

For a thin SiGe well, nevertheless, the ground state in the well will shift away from the valence band edge because of carrier confinement (Cohen-Tannoudji, Diu, & Laloe, 1977). In order to calculate the energy levels and sub-bands in terms of quantum well's profile (Ge content and layer thickness) the Schrödinger equation has to be solved for holes in the valence band using  $6 \times 6$  Luttinger Hamiltonian. These theoretical calculations can be essential for designing structures for high TCR values.

#### 1.4 Signal-to noise ratio

Noise for an electronic signal is a stochastic random variation which makes it difficult to distinguish the signal amplitude and as a result the IR detectivity becomes limited. The noise occurs when the voltage or current measurements are performed for a device and it is the summation of contributions from the different sources. These sources can be divided into two main groups; a) external or extrinsic sources which are generated due to the surrounding performance of the device and b) Internal or intrinsic sources which refers to random fluctuation in the carrier transport because of defects and imperfections in the device structure.

The thermal noise (it is also so-called Nyquist or Johnson noise) is similar as Brownian motion of the charged carriers in a material and its nature is a random thermal motion. In a conductive material, at non-zero temperature  $T$ , electrons vibrate randomly depending on  $T$ . This noise is expressed for a resistor  $R$  in a  $\Delta f$  bandwidth by:

$$V_J^2 = 4kTR\Delta f \quad (10)$$

where  $k$  is the Boltzmann constant. This means that the thermal noise can be minimized for bolometer application by lower resistive material, lower operating temperature and narrower bandwidth. However, an actual bolometer application requires a finite limit to the bandwidth through the scanning and readout of the detectors and ambient temperature operation. Thermal or temperature fluctuation noise is another noise source which must be discussed to evaluate the detectivity of the device.

Since the detector consists of an array of pixels which are suspended membranes, and has legs connected to the ROIC, then a thermal or temperature fluctuation noise is created which affects the detectivity of the device. This will transform in a form of an electric noise because of the coupling between the temperature and the resistance. Temperature fluctuation is expressed as follows (Kruse et al., 1962; Smith et al., 1968):

$$V_{th}^2 = \frac{4kT^2\Delta f}{(1 + \omega^2\tau_{th}^2)^{1/2}} K^2 R_{th} \quad (11)$$

The other important source of noise for IR detection is the “background noise”. Heat exchange due to radiation between the detector at temperature  $T_d$  and the environment at temperature  $T_b$  generate voltage noise which is so called “background noise”. As an example an exchange of the heat between the sensitive area of the detector and the surrounding substrate and contact legs (which are in thermal contact with the detector) introduces a random fluctuation in the temperature. This will then transform into a kind of electric noise because of the coupling between the temperature and the resistance. The expression is given by (Kruse et al., 1962; Smith et al., 1968):

$$V_b^2 = \frac{8k\varepsilon\sigma A(T_d^2 + T_b^2)}{1 + \omega^2\tau_{th}^2} K^2 R_{th}^2 \quad (12)$$

where  $\varepsilon$  is emissivity,  $\sigma$  is Stefan-Boltzmann constant and  $A$  is the area of the detector. For semiconductor thermal detectors,  $1/f$  noise or Flicker Noise is the most predominant noise at low frequency.  $1/f$  noise can be evaluated by noise constant:  $K_{1/f} = \gamma/N$  where  $\gamma$  is known as the Hooge's constant and  $N$  is the total number of free charges (Hooge, 1994). The exact description for the origin of  $1/f$  noise is not clear but the interactions of carriers with defects, surface states and other events (e.g. recombination and trapping-detrapping) are the major causes of this noise in semiconductors. In the case of bolometers, a simple expression for voltage power spectrum density (PSD) can be written as follows:

$$S_V = \frac{K_{1/f} V_{bias}^\beta}{f^\gamma} \quad (13)$$

where  $K_{1/f}$  is a noise constant. In a similar way,  $1/f$  noise voltage can be written as:

$$V_{1/f}^2 = \frac{K_{1/f} I^\beta}{f^\gamma} \Delta f \quad (14)$$

The parameters  $\gamma$ ,  $\beta$  and  $K_{1/f}$  in equations 13 and 14 are dependent on the material, processing, metal contacts and surfaces and thus, very difficult to calculate analytically (Hooge, 1994). Since  $1/f$  noise relates to defects and imperfections in the active part of the bolometer, it is believed that using single-crystalline (sc) materials will demonstrate low noise constant in comparison to polycrystalline or amorphous ones. Thus, a solution for increasing the  $D^*$  of a bolometer is to use mono-crystalline temperature sensing bolometer materials with a low  $1/f$  noise constant (Kolahdouz, Afshar Farniya, Di Benedetto, & H. Radamson, 2010).

For most bolometer applications, the frequency exponent  $\gamma$  in equations 13 and 14 is close to 1. The square of total noise voltage for a thermistor material in active part of a bolometer may be formulated in eq as:

$$V_J^2 = V_J^2 + V_{th}^2 + V_b^2 + V_{1/f}^2 \quad (15)$$

When a thermal detector absorbs the electromagnetic radiation, both output signal and noise will be generated. High amplitude output signal and low noise level are desired in an infrared detector. To evaluate the performance of the detector, "Detectivity" may be defined as follow:

$$D = \frac{R_V}{\Phi_0} = \frac{V_s}{\Phi_0 V_n} \quad (16)$$

where  $V_n$ ,  $V_s$  and  $\Phi_n$  are RMS signal voltage, noise voltage, and incident power respectively.

The detectivity is proportional to detector area and electrical bandwidth. Therefore, the normalized detectivity  $D^*$  is given by:

$$D^* = D \times A^{1/2} \times \Delta f^{1/2} \quad (17)$$

In a thermal detector,  $D^*$  can be expressed as:

$$D^* = \frac{K\varepsilon R_{th} A^{1/2}}{(1 + \omega^2 \tau_{th}^2)^{1/2} (V_J^2 + V_{th}^2 + V_b^2 + V_{1/f}^2)^{1/2}} \quad (18)$$

where  $A$  is the pixel area. From eq. 16, it can be concluded that the detectivity may be enhanced by increasing the responsivity and/or decreasing the noise. The responsivity, like the Flicker noise, increases linearly with voltage, while the Johnson noise is independent of voltage. At small voltages, the noise is mainly Johnson noise. But, at sufficiently high  $V$ , noise is dominated by the Flicker noise and  $D^*$  is independent of voltage. According to the previous calculations, the highest detectivity for a thermal detector at room temperature and viewing background at room temperature is about  $2 \times 10^{10} \text{ cmHz}^{1/2} \text{ W}^{-1}$  which can be referred to as the thermal detectors theoretical limitation. The published photon detectors have shown higher detectivities as a result of their limited spectral responses.

In addition to the above discussions, the importance of the electrical contacts' influence on the thermistor's performance has to be emphasized. The current-voltage characteristics of the thermistor materials are greatly influenced by the nature of the metal/silicide-semiconductor interface. Ohmic contact with low contact resistance is the requirement for low noise level for many applications. However, when large electrical current is involved a low sheet resistance contact is required to make the current flow uniform without localized overheating. A metal with low work function will form an ohmic contact to an n-type semiconductor with surface states. The reverse story is true for a p-type semiconductor. In these cases, introducing higher doping concentration reduces the contact resistance near the contact surface (barrier thinning).

## 2. Noise measurement of the thermistor materials

Power spectral density (PSD) of voltage noise is measured for different pixels. The measurements can be performed at different temperatures inside a shielded probe station to avoid light and the environmental noise. The frequency range is usually 0.3-10,000 [Hz] with some sub-intervals. Each final PSD vs frequency curve includes many thousands of data. Fig. 4 shows the experimental set up. The device is biased through a circuit isolated by a metallic box.

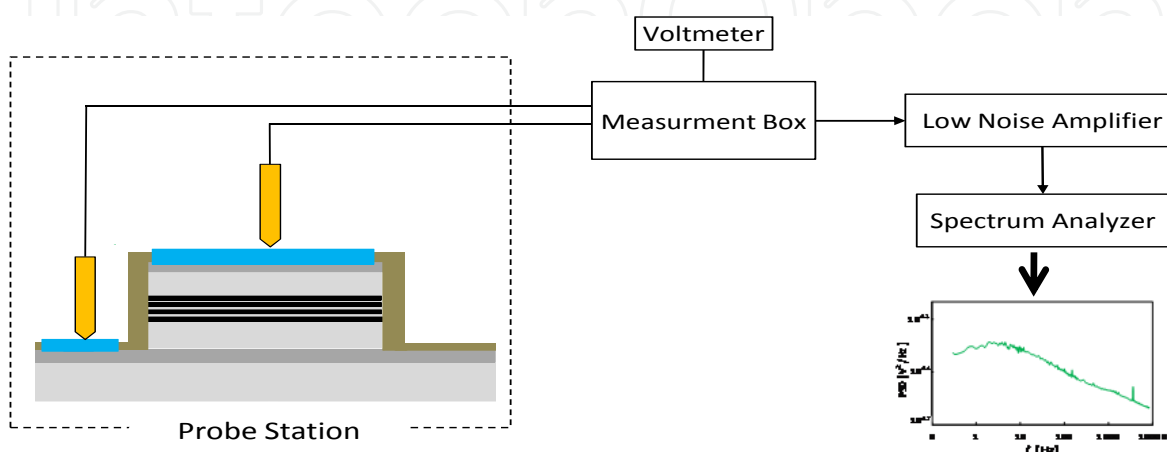


Fig. 4. Experimental set up for measuring PSD of voltage noise.

## 3. Thermistor materials for uncooled bolometers

Bolometers are uncooled detectors and today they have dominantly taken over the IR market. Among the existing thermistor materials, Vanadium oxide ( $\text{VO}_x$ ) is mainly used for bolometer applications and its performance has been studied and improved during many years. Nowadays, it is believed that  $\text{VO}_x$  technology will be challenged in the near future by the new silicon based materials due to their low cost structure, and easier manufacturability (Rogalski, 2011).

In this part, an overview of the  $\text{VO}_x$  material properties is presented and later, the discussions will be extended towards single-crystalline Si-based materials.

### 3.1 Vanadium oxide

Vanadium oxides are the most popular thermistor material in fabrication of today's IR detectors. This material is grown by different techniques e.g. sputtering (Y. Han et al., 2003; Lv et al., 2007; Moon, Y. Han, K. Kim, S. Lee, & Shin, 2005), reactive e-beam evaporation (Subrahmanyam, Bharat Kumar Redd, & Nagendra, 2008), reactive e-beam evaporation (H. Wang, Yi, & Chen, 2006), PLD (Kumar et al., 2003), and CVD (Mathur, Ruegamer, & Grobelsek, 2007). Many reports demonstrate that by tuning the growth parameters, a transition occurs from amorphous to nano-crystalline FCC  $\text{VO}_x$  ( $0.8 < x < 1.3$ ) (Cabarcos et al., 2011).

Since vanadium atom has a half-filled d-shell, there exist a set of valence states to form a number of oxide phases. The typical phases are known as VO,  $\text{V}_2\text{O}_3$ ,  $\text{VO}_2$  (or  $\text{V}_2\text{O}_4$ ) and  $\text{V}_2\text{O}_5$  (or as a "mixed oxide") (Subrahmanyam et al., 2008).

Among these phases,  $V_2O_3$  shows semiconductor-to-metal transition at  $\sim 160K$  and demonstrates a very low resistance. For bolometer application,  $VO_2$  phase is typically used due to its high TCR value but its metal transition temperature occurs at  $\sim 341 K$  which restricts the bolometer's IR detection. Another interesting vanadium oxide is  $V_2O_5$ . This phase shows a good TCR; however, its resistance is very high resulting in high noise value.

Thus, a mixed phase of  $VO_2$  and  $V_2O_5$  may demonstrate an appropriate resistivity which is convenient and matches also with the readout electronics for high sensitive bolometers (Malyarov, 1999).

The growth of  $VO_x$  films requires extra care since the morphology of the film is sensitive to the growth parameters. In most cases, the substrate temperature and the oxygen pressure are the two crucial growth parameters to control the composition and the grain size of the oxide films. The grown  $VO_x$  films demonstrate TCR values in range of 2 -3% $K^{-1}$ . Some of the published data are addressed in table 1.

Technique	Material	Processing temperature (K)	TCR ( $K^{-1}$ )	References
Dc sputtering+oxidation	$VO_x$	673	2.0	Chen et al
PLD	$VO_x$	300	2.8	Rajendra Kumar et al
Ion beam sputtering+ oxidation	$VO_2$	473	2.6	Wang et al
RF sputtering	$V_2O_5 / V / V_2O_5$	573	2.6	Moon et al
RF sputtering	V-W-O	573	2.6	Han et al
dc magnetron sputtering+annealing	$VO_2$	673	4.4	Yuqiangwt al
Reactive e-beam evaporation	$VO_2 + V_2O_5$	473	3.2	Subrahmanyam et al

Table 1. A summary of different deposition techniques for the growth of vanadium oxide with the process temperature and the reported TCR values.

A lot of efforts were being made to improve the quality of resistive  $VO_x$  films and to obtain TCR values above 3% $K^{-1}$ . The success was achieved by introducing tungsten-doping in a multilayer structure of  $V_2O_5$  (Y. H. Han, S. H. Lee, K. T. Kim, I. H. Choi, & Moon, 2007; Y. Han, 2003; Moon, 2005). These oxide layers were deposited by reactive dc sputtering followed by an annealing treatment (673K). The analysis showed a TCR value of  $\sim -4.4\% \text{ } ^\circ K^{-1}$  and a sheet resistance of 20 k  $\Omega$ /square (Dai, X. Wang, He, Huang, & Yi, 2008; Lv et al., 2007). Although these results indicate a breakthrough for material performance, this material is not suitable for micro-machining process on Si and the fabrication of bolometers due to high temperature budget.

As discussed above, the  $1/f$  noise is also an important figure of merit for thermistor materials. The noise in the oxide layers is caused mainly from the induced mechanical stresses due to the large grain sizes in the mixed phases. Zerov *et al* (Zerov, 2001) showed that the noise level in the oxide films is originated from two principal parameters: the concentration of different phases of  $VO_x$  and the grain size.

A recent study shows that high tungsten contents in vanadium oxide films (alloys of  $V_{1-x}W_xO_2$  or VWO) will improve the thermal performance of the oxide material. Takami et al

(Takami, Kawatani, Kanki, & Tanaka, 2010) showed that the TCR performance of  $V_{1-x}W_xO_2$  films grown on  $Al_2O_3(0001)$  depends strongly on tungsten content. The tungsten level has been optimized and  $V_{0.85}W_{0.15}O_2$  demonstrates a TCR value of 10%/K at room temperature. Moreover, the TCR behavior is found to be almost independent of layer thickness which is very beneficial for bolometric application.

### 3.2 Single-crystalline Si(C)/SiGe(C) multilayer structures

Many initiatives were taken to improve the IR detection and to obtain high quality imaging. Most of these efforts have striven to increase SNR and the thermal response of the detector. For bolometers,  $1/f$  noise is the main source of noise (Lv et al., 2007).

Single crystalline semiconductor heterostructures are outstanding alternatives for low noise thermistor material. Among low cost semiconductor materials, SiGe(C)/Si(C) MQWs are the most appealing alternatives due to its low noise performance. This material system is therefore very promising for future mass-market applications. The structures demonstrate low noise when high quality of epi-layers, interfacial roughness (or unevenness) and the contact resistances are obtained (Kolahdouz, Afshar Farniya, Di Benedetto, et al., 2010; Kolahdouz, Afshar Farniya, Östling, & H. Radamson, 2010).

When the semiconductor thermistor material is heated, thermal excitations generate carriers (holes in this case) which have energies high enough to overcome the potential barrier of the quantum well. If a voltage is applied across the active region, these excited carriers move in the direction of the applied field, thus resulting in a current (see Fig. 5). This current increases at higher temperatures by increasing the number of the carriers in the current stream.

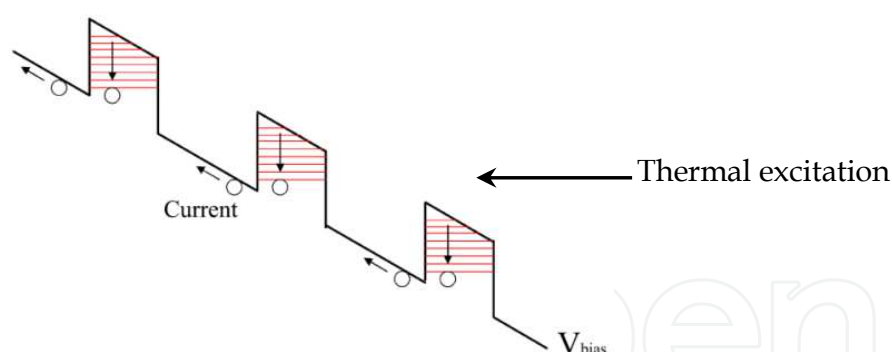


Fig. 5. When a voltage is applied across the thermistor, the valence band in SiGe/Si is tilted and thermally excited holes move towards the negative potential.

Kolahdouz et al. (Kolahdouz, Afshar Farniya, Di Benedetto, et al., 2010) presented the effect of Ge content (barrier height) on the performance of the SiGe/Si multi quantum wells (MQWs) and dots (MQDs) as thermistor material. In this study three Ge contents (23, 28 and 32%) in SiGe wells were applied and for higher Ge content (~47%), Ge-dots/Si systems were grown. In order to have a decent growth rate, the samples were grown at 600 °C. At this growth temperature, the intermixing of Si into Ge makes it impossible to grow pure Ge dots. This problem makes these structures vulnerable to strain relaxation and defect formation.

The experimental data demonstrated a TCR value of  $\sim 3.4\%K^{-1}$  for Ge MQDs which is a clear improvement compared to SiGe wells layers with  $2.7\%K^{-1}$ . However, a remarkable increase of the noise constant ( $k_{1/f}$ ) is observed for MQDs compared to MQWs (see Fig.6). It is believed that the noise level is sensitive to the variation of hole concentration in the Ge-dot systems' structures compared to the uniform profile in SiGe wells. Any strain relaxation in Ge dots will contribute to the noise level. A summary of both MQW and MQD SiGe/Si is presented in table 2.

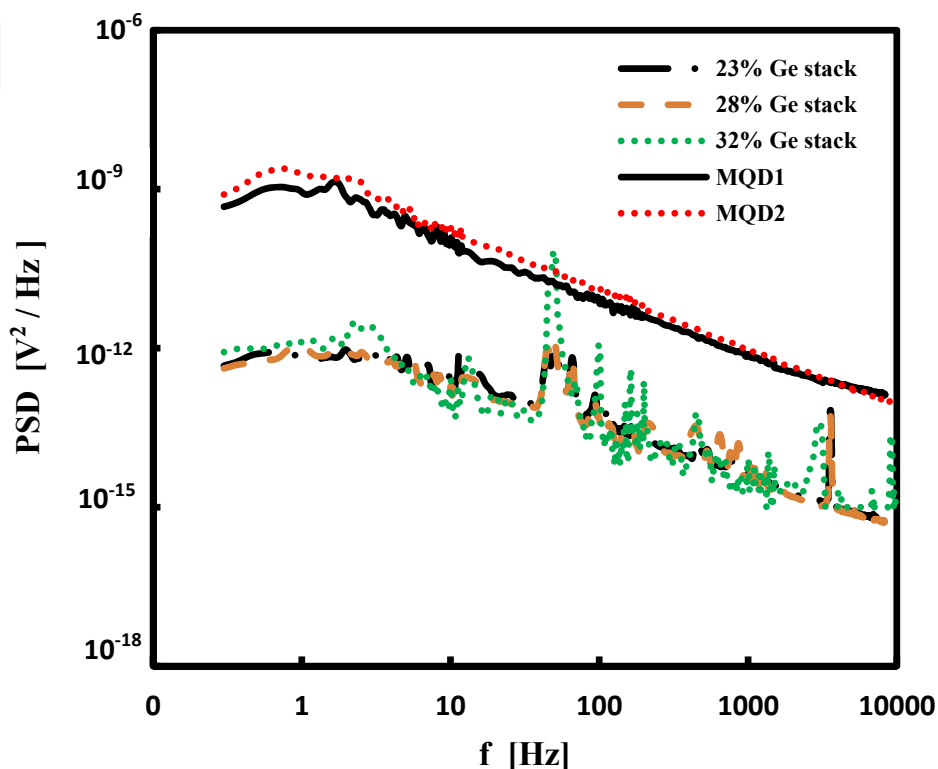


Fig. 6. Noise power spectral density of devices vs. frequency for pixel area  $70 \times 70 \mu m^2$  in Si/SiGe MQWs and MQDs.

	Ref. Si	MQW1	MQW2	MQW3	MQD1	MQD2
Ge content (%)	0	23	28	32	47	>47
Estimated barrier height (eV) <sup>a</sup>	...	0.19	0.23	0.27	...	...
TCR (%/K) for $200 \times 200 \mu m^2$	0.12	1.39	1.87	2.42	2.51	2.87
TCR (%/K) for $140 \times 140 \mu m^2$	0.09	1.55	2.06	2.50	2.86	3.14
TCR (%/K) for $100 \times 100 \mu m^2$	0.08	1.66	2.15	2.55	2.92	3.23
TCR (%/K) for $70 \times 70 \mu m^2$	0.08	1.70	2.77	2.57	2.98	3.4
$K_{1/f}$	$9 \times 10^{-13}$	$1 \times 10^{-12}$	$3 \times 10^{-12}$	$4.4 \times 10^{-12}$	$2 \times 10^{-9}$	$2 \times 10^{-9}$
Energy quantized levels (meV)	...	9.6,38,54,84.1,84.2	10.1,40,62,89,94	10.4,41,68,92,101	...	...
Normalized resistance ( $\Omega mm^2$ ) ( $R_0=R \times area = \rho \times l$ )	0.2	1.17	3.46	2.39	2.91	4.88

Table 2. Summary of estimated barrier heights, TCR(%/K),  $K_{1/f}$ ,  $R_0$ , and energy levels in QWs (at room temperature) for all sizes of detector structures. Due to partial strain relaxation, the barrier height of the quantum dots is not specified.

These results indicate that the performance of the thermistor material SiGe/Si MQWs (or MQDs) is very sensitive to structure profile.

Andersson et al, (J. Y. Andersson, P. Ericsson, H. H. Radamson, S. G. E. Wissmar, & Kolahdouz, 2011) presented theoretical calculations to optimize TCR in terms of the Ge content and quantum well width in SiGe/Si MQW and MQD systems (see Fig.7). The results were also compared to the experimental data. The extracted TCR values for MQW structures showed that the thermal response of detectors increases with Ge content which is consistent with the experimental data. The authors propose Ge dots with high Ge content as a better solution for SiGe wells. The valence band off-set and TCR values versus the size of Ge dots were calculated (see Fig.8a). The ground level energy relative valence band edge in Si versus the quantum dots demonstrates the dependency of TCR on the size of Ge dots (see Fig.8b). The results show that dots with 60 nm could exhibit a TCR value of 8.5% which is excellent for IR detection. However, these calculations do not consider the noise level in MQD system. The growth of pure Ge dot on the Si surface is a challenging task due to the intermixing of Si into Ge. In order to avoid this problem, low temperature epitaxy can be applied to grow Ge dots with high Ge content in MQD structures. This low temperature process suffers from low growth rate and thus makes it impractical for mass production.

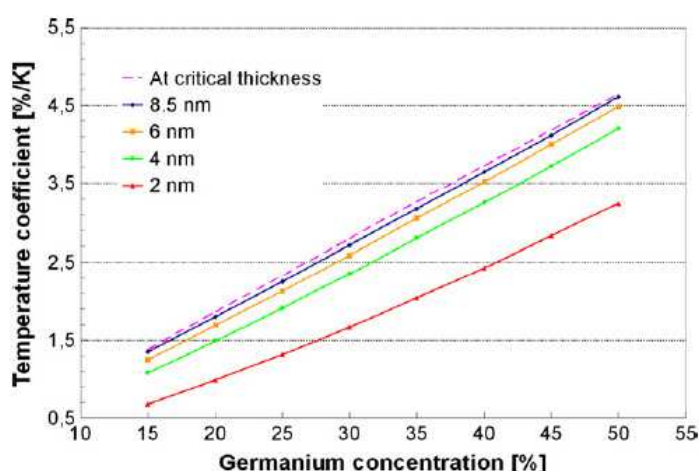


Fig. 7. The temperature coefficient versus Ge content in the QWs, for different QW widths. simulated data.

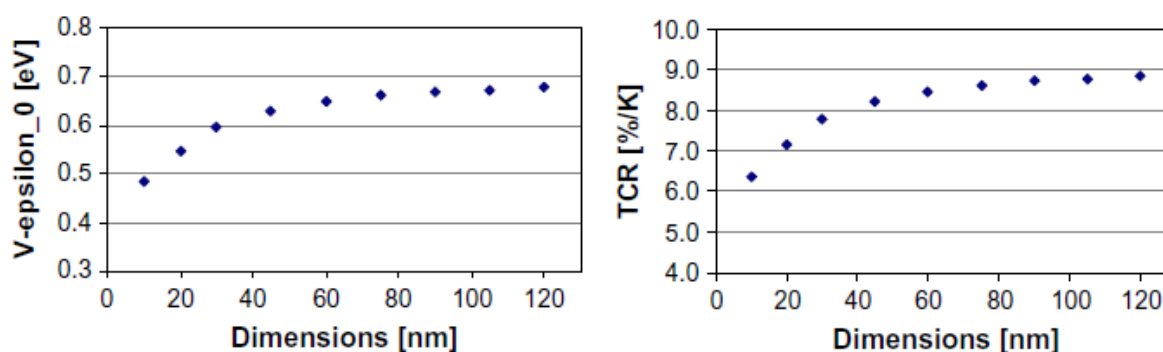


Fig. 8. a. Plots of ground level energy relative valence band edge in Si for different Ge dot sizes, and b. the dependence of the temperature coefficient of resistivity (TCR) on dot size.

Wissmar et al. (S. Wissmar et al., 2006) investigate the TCR performance of SiGe/Si and AlGaAs/GaAs systems. This study also demonstrates the dependence of thermal performance of MQW structures versus the quantum well profile (composition, dopant concentration and the width of the quantum wells). The performance of the structures is degraded with increasing the dopant concentration in the quantum well. The AlGaAs/GaAs system demonstrates excellent performance (4.5%/K) compared to SiGe/Si system (2 %/K). However, the low cost Si technology is always preferred over III-V for industrial applications.

More discussions about the SiGe/Si thermistor material are presented by Ericsson et al. (Per Ericsson et al., 2010) It is generally observed that the flicker noise is volume dependent (Motchenbacher, 1973). This study presents the effect of pixel area on the Flicker noise (the vertical thickness is constant). The data show the dependency of  $1/A$  as expected by theories (see Fig. 9).

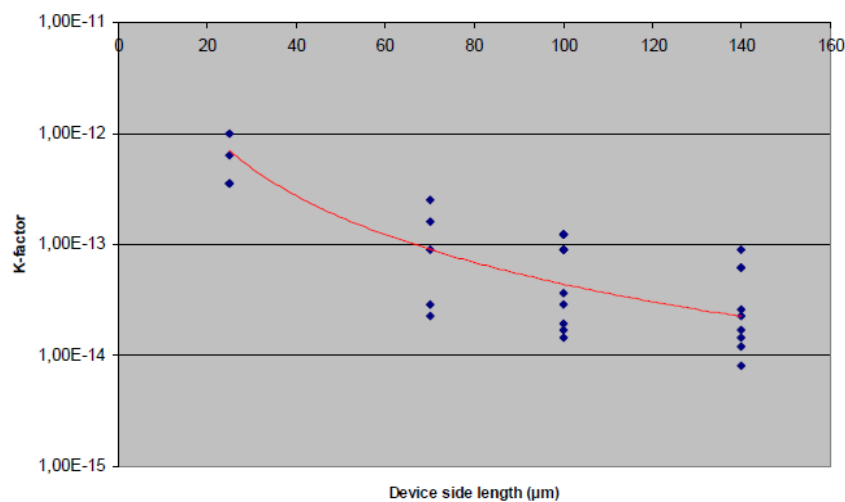


Fig. 9. The flicker noise k-value for SiGe/Si MQW structures with different pixel sizes and the predicted variation (solid line). All data have been manufactured on the same wafer.

A vital issue in many cases for bolometers containing SiGe/Si MQW system is the control of the residual strain in the suspended membrane.

Radamson et al. (H. H. Radamson, Kolahdouz, Shayestehaminzadeh, Afshar Farniya, & S. Wissmar, 2010) reports the integration of C in the Si/SiGe stack (SiGe(C) / Si(C) MQWs) to create alternating tensile/compressive strain systems. The SiGe(C) layers were created through the intermixing of Si into the embedded Ge thin layers (grown by introducing GeH<sub>4</sub> without SiH<sub>4</sub>). The intermixing of Si and Ge can be controlled by the growth temperature and the carbon doping in the Si barrier layer (Hirano & Murota, 2009). This study compares five different structure profiles considering the effect of contact resistance (Ni silicide contacts), Ge content, and carbon doping in Si barrier (see Table 3). The prototypes exhibited an outstanding TCR of 4.5%/K for 100×100μm<sup>2</sup> pixel sizes and low noise constant ( $K_{1/f}$ ) value of  $4.4 \times 10^{-15}$ . The excellent performance of the devices was due to low contact resistance in presence of Ni silicide contacts, smooth interfaces, and high quality multi quantum wells (MQWs) containing high Ge content. Fig.10 demonstrates the noise data for the samples described in table 3. Samples MQW1 (no silicide contacts) and MQW5 (Si<sub>0.35</sub>Ge<sub>0.65</sub>/SiC with silicide contacts) show the highest and the lowest noise level among this sample series.

	MQW1	MQW2 (silicide)	MQW3 (C in barrier)	MQW4 (Ge-delta+silicide)	MQW5 (Ge-delta+ silicide+C in barrier)
Ge content[%]	28	28	>28	10	65
Estimated barrier height (eV) <sup>9</sup>	0.23	0.23	0.23	0.07	0.5
Activation energy (eV) for 100×100μm <sup>2</sup>	0.17	0.18	0.19	0.07	0.35
TCR [%/K] for 200×200μm <sup>2</sup>	1.87	2.32	2.75	0.6	4
TCR [%/K] for 100×100μm <sup>2</sup>	2.77	2.30	2.78	1.07	4.5
K <sub>1/f</sub> for 100×100μm <sup>2</sup>	4.1×10 <sup>-12</sup>	1.4×10 <sup>-13</sup>	5×10 <sup>-14</sup>	8.5×10 <sup>-15</sup>	4.4×10 <sup>-15</sup>
Normalized Resistance [Ωmm <sup>2</sup> ] (R <sub>0</sub> =R×area=ρ×l)	3.46	2.67	19.66	0.4	3.11

Table 3. Summary of estimated barrier heights, TCR [%/K], K<sub>1/f</sub> and R<sub>0</sub> in MQWs (at room temperature) for all sizes of detector.

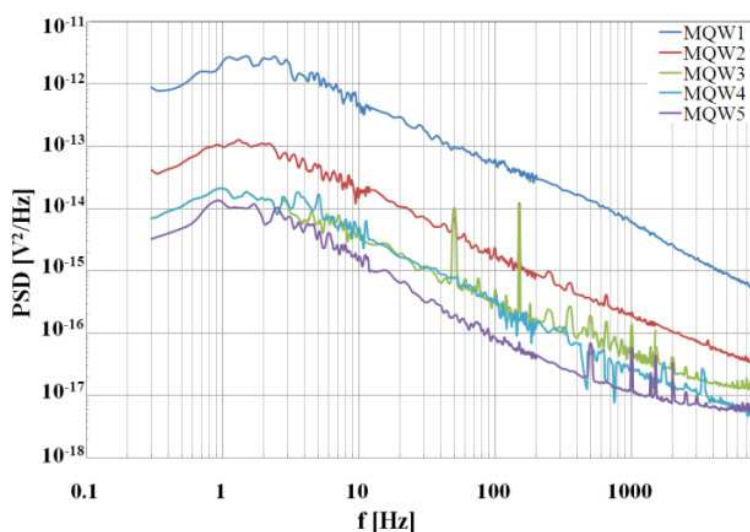


Fig. 10. Noise power spectral density of devices vs. frequency for pixel area 100×100 μm<sup>2</sup> in SiGe MQWs described in table 3.

#### 4. Fabrication process flow

Bolometers are mainly composed of a temperature sensing resistor and an IR absorber. A good thermal isolation is the requirement to increase the sensitivity of these detectors. This can be achieved by suspending the bolometer structure in the air through either membrane or bridge support as shown in Fig. 11.

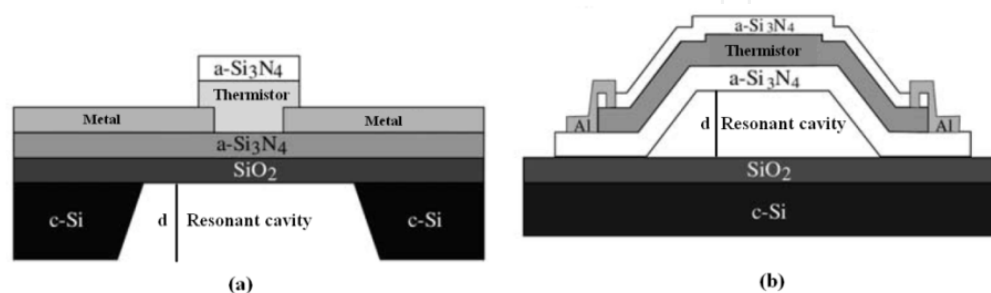


Fig. 11. Cross-section of a) the membrane-supported and b) the bridge-supported microbolometer (Garcia, 2004).

It was reported in 2004 (Garcia, 2004) that the noise current of the bridge-supported structures is one order of magnitude higher than that of the membrane-supported structure. However, the bridge-supported structure process flow enables a precise control on the resonant cavity length which makes it the dominant design for microbolometers.

The process flow of fabricating a bolometer is very dependent on the thermistor material. For thermistors which may be deposited at low temperatures, there is a possibility of being directly integrated on the readout integrated circuit (ROIC) without harming its elements. Amorphous Si, SiGe, Ge,  $\text{Ge}_x\text{Si}_{1-x}\text{O}_y$  and poly  $\text{VO}_x$  material are a few examples of such thermistors. The advantage of the mentioned group IV-based materials in this list is their absolute compatibility with the silicon processing line.

The process flow is described in Fig. 12 (Mottin et al., 2002). It is the simplest manufacturing method in which the thermistor material can be grown directly on ROIC. The first step is the deposition of a thin reflective layer directly on top of the ROIC. A thick sacrificial layer is then spun and cured to form the resonant cavity at the end of the process. The thermistor material is deposited over the sacrificial layer and covered by the metallic contact electrodes. The metallic contact deposition and etching enable electrical continuity between the underlying substrate and the thermistor on the surface of the sacrificial layer. Finally, the micro-bridge arrays are released by removing the sacrificial layer.

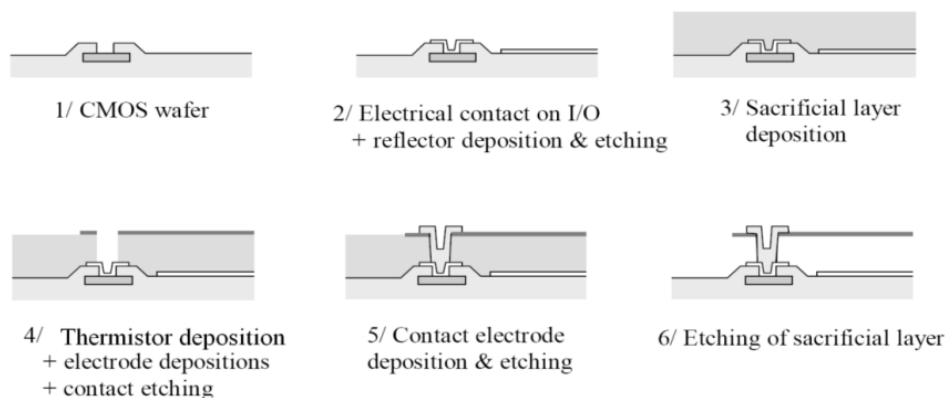


Fig. 12. Process flow of a bridge-supported microbolometer technology (Mottin et al., 2002).

The second fabrication method is based on wafer bonding where thermistor material is transferred from epi-wafer to ROIC wafer. This is necessary since a thermal treatment (850-900 C) is required for in-situ cleaning prior to epitaxy of single-crystalline layers. A process flow for fabrication of bolometers based on structures composed of sc- group IV materials through wafer bonding process on ROICs (Kvisterøy et al., 2007; J. Källhammer et al., 2006; F. Niklaus et al., 2001) is demonstrated in Fig. 13. In this process, group IV-based structures are deposited on a separate SOI carrier wafer and are then transferred from the handle wafer to the ROIC wafer using low-temperature adhesive wafer bonding in combination with sacrificial removing of the carrier wafer. The advantage of 3D bolometer integration is that it allows the employment of high TCR and SNR mono-crystalline thermistor for imaging applications.

For many detector applications, Ni is chosen as the absorbent layer. This is due to its simple preparation and the fact that it can get a strong absorption of about 90% in wavelength range between 7-13  $\mu\text{m}$  (Lienhard, Heepmann, & Ploss, 1995). In 2006 Hsieh et al. (Hsieh, Fang, & Jair, 2006) reported TCR value of  $-2.74\% \text{K}^{-1}$  and activation energy of 0.21eV for  $\text{Si}_{0.68}\text{Ge}_{0.31}\text{C}_{0.01}$  ternary system.

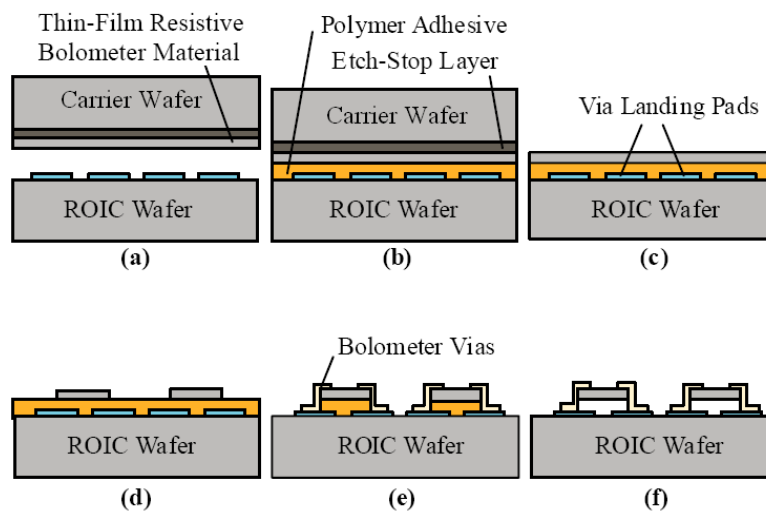


Fig. 13. A Schematic picture of a Si-based bolometer process (F. Niklaus et al., 2007).

The sc-SiGe/Si structure is transferred to the ROIC by low temperature adhesive wafer bonding and subsequent removal of the carrier. In 2010, Lapadatu et al. (Lapadatu et al., 2010) proposed a novel approach to increase the fill factor. In their design the legs, which support the bolometer membrane and connect it to the ROIC, are built underneath the membrane as shown in Fig. 14.

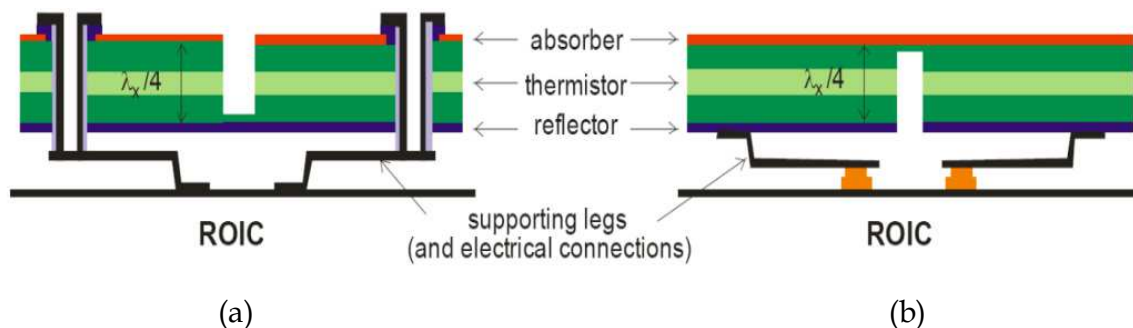


Fig. 14. Schematic representation of the bolometer pixel illustrating two schemes for electrical connection (Lapadatu et al., 2010) (a) through-pixel plugs; (b) under-pixel plugs.

It was reported that the detectors composed of SiGe quantum wells have presented a TCR around  $3.1\%K^{-1}$  and  $5 \times 10^{-13}$  for  $K_{1/f}$  (Lapadatu et al., 2010).

It is important to emphasize here that the recent advanced cleaning technique together with new gas precursor for Si (trisilane) and Ge (digermane) may provide the opportunity to grow epi-layers at low temperatures (300-500 °C). This means that the fabrication technique will become similar to the steps in Fig.12 and sc-Si-based material will be deposited directly on ROIC wafer.

## 5. Conclusions

Among different materials, single crystalline SiGe alloy is a promising thermistor material in bolometers for LWIR detections. The temperature response of SiGe/Si multi quantum well (or dot) structures depends mainly on Ge content (strain). The signal-to-noise ratio which is

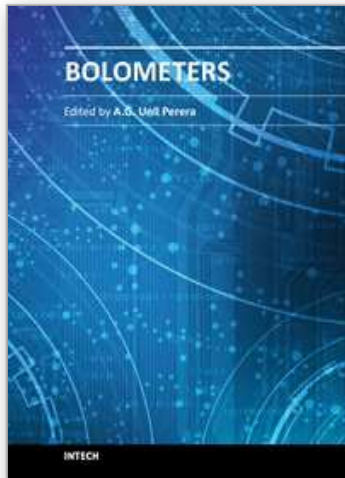
an important parameter for thermal imaging is strongly sensitive to contact resistance, interfacial and layer quality of SiGe layers. It is demonstrated that carbon-doping impedes the defect formation in SiGe layers and SiGe(C)/SiC with Ni silicide contacts is the most attractive structure for high performance bolometers.

## 6. References

- Andersson, J. Y., Ericsson, P., Radamson, H. H., Wissmar, S. G. E., & Kolahdouz, M. (2011). SiGe/Si quantum structures as a thermistor material for low cost IR microbolometer focal plane arrays. *Solid-State Electronics*, 60(1), 100-104. Elsevier Ltd. doi:10.1016/j.sse.2011.01.034
- Bean, J. C., Feldman, L. C., Fiory, A. T., Nakahara, S., & Robinson, I. K. (1984). Ge<sub>x</sub>Si<sub>1-x</sub> strained-layer superlattice grown by molecular beam epitaxy. *J. Vac. Sci. Technol. A*, 2(2), 436-440.
- Di Benedetto, L., Kolahdouz, M., Malm, B. G., Ostling, M., & Radamson, H. H. (2009). Strain balance approach for optimized signal-to-noise ratio in SiGe quantum well bolometers. *ESSDERC 2009 - Proceedings of the 39th European Solid-State Device Research Conference* (pp. 101-104).
- Cabarcos, O. M., Li, J., Gauntt, B. D., Antrazi, S., Dickey, E. C., Allara, D. L., & Horn, M. W. (2011). Comparison of ion beam and magnetron sputtered vanadium oxide thin films for uncooled IR imaging. *Proc. of SPIE Vol. 8012* (Vol. 8012, p. 80121K-80121K-9). doi:10.1117/12.884377
- Cohen-Tannoudji, C., Diu, B., & Laloe, F. (1977). *Quantum Mechanics*. New York, USA: John Wiley and Sons.
- Dai, J., Wang, X., He, S., Huang, Y., & Yi, X. (2008). Low temperature fabrication of VO<sub>x</sub> thin films for uncooled IR detectors by direct current reactive magnetron sputtering method. *Infrared Physics & Technology*, 51(4), 287-291. doi:10.1016/j.infrared.2007.12.002
- Ericsson, Per, Höglund, Linda, Samel, B., Savage, Susan, Wissmar, Stanley, Oberg, O., Kallhammer, J.-E., et al. (2010). Design and evaluation of a quantum-well-based resistive far-infrared bolometer. *Proc. of SPIE Vol. 7834* (Vol. 7834, pp. 78340Q1-10). doi:10.1117/12.865036
- Garcia, M. (2004). IR bolometers based on amorphous silicon germanium alloys. *Journal of Non-Crystalline Solids*, 338-340, 744-748. doi:10.1016/j.jnoncrysol.2004.03.082
- Han, Y. H., Lee, S. H., Kim, K. T., Choi, I. H., & Moon, S. (2007). Properties of electrical conductivity of amorphous tungsten-doped vanadium oxide for uncooled microbolometers. *Solid State Phenom.*, 343, 124-126.
- Han, Y., Choi, I., Kang, H., Park, J., Kim, K., Shin, H., & Moon, S. (2003). Fabrication of vanadium oxide thin film with high-temperature coefficient of resistance using V<sub>2</sub>O<sub>5</sub>/V/V<sub>2</sub>O<sub>5</sub> multi-layers for uncooled microbolometers. *Thin Solid Films*, 425(1-2), 260-264. doi:10.1016/S0040-6090(02)01263-4
- Hirano, T., & Murota, J. (2009). A Study on Formation of Strain Introduced Group IV Semiconductor Heterostructures by Atomic Layer Doping. *Record of Electrical and Communication Engineering Conversation Tohoku University*, 78(1), 407-8.
- Hooge, F. N. (1994). 1/F Noise Sources. *IEEE Transactions on Electron Devices*, 41(11), 1926-1935. doi:10.1109/16.333808
- Hsieh, M., Fang, Y. K., & Jair, D. K. (2006). The study of a novel crystal SiGeC far infrared sensor with thermal isolated by MEMS technology. *Microsystem Technologies*, 12(10-11), 999-1004. doi:10.1007/s00542-006-0162-7

- Kolahdouz, M., Afshar Farniya, A., Di Benedetto, L., & Radamson, H. (2010). Improvement of infrared detection using Ge quantum dots multilayer structure. *Applied Physics Letters*, 96(21), 213516. doi:10.1063/1.3441120
- Kolahdouz, M., Afshar Farniya, A., Östling, M., & Radamson, H. (2010). Improving the performance of SiGe-based IR detectors. *ECS Transactions*, 33 (6) (Vol. 33, pp. 221-225).
- Kruse, P. W., McGlauchlin, L. D., & McQuistan, R. B. (1962). *Elements of Infrared Technology. Generation, transmission, and detection*. Wiley, New York, (Vol. 137, pp. 123-123). Wiley, New York. doi:10.1126/science.137.3524.123
- Kumar, R. T. R., Karunagaran, B., Mangalaraj, D., Narayandass, S. K., Manoravi, P., Joseph, M., & Gopal, V. (2003). Study of a pulsed laser deposited vanadium oxide based microbolometer array. *Smart Materials and Structures*, 12(2), 188-192. doi:10.1088/0964-1726/12/2/305
- Kvisterøy, T., Jakobsen, H., Vieider, C., Wissmar, S., Ericsson, P., Halldin, U., Niklaus, Frank, et al. (2007). Far infrared low-cost uncooled bolometer for automotive use. *Proc. AMAA*. Berlin, Germany.
- Källhammer, J., Pettersson, H., Eriksson, D., Junique, S., Savage, S., Vieider, C., Andersson, J. Y., et al. (2006). Fulfilling the pedestrian protection directive using a long-wavelength infrared camera designed to meet both performance and cost targets. *Proceedings of SPIE*, 6198, 619809-1. Spie. doi:10.1117/12.663152
- Lapadatu, A., Kittilsland, G., Elfving, A., Hohler, E., Kvisterøy, T., Bakke, T., & Ericsson, P. (2010). High-performance long wave infrared bolometer fabricated by wafer bonding. *Technology*, 7660, 766016-766016-12. doi:10.1117/12.852526
- Liddiard, K. C. (1984). Thin-film resistance bolometer IR detectors. *Infrared Physics*, 24(1), 57-64. doi:10.1016/0020-0891(84)90048-4
- Lienhard, D., Heepmann, F., & Ploss, B. (1995). Thin nickel films as absorbers in pyroelectric sensor arrays. *Microelectronic Engineering*, 29, 101-104.
- Lv, Y., Hu, M., Wu, M., & Liu, Z. (2007). Preparation of vanadium oxide thin films with high temperature coefficient of resistance by facing targets d.c. reactive sputtering and annealing process. *Surface and Coatings Technology*, 201(9-11), 4969-4972. doi:10.1016/j.surfcoat.2006.07.211
- Malyarov, V. G., Khrebtov, I. A., Kulikov, Y. V., Shaganov, I. I., Zerov, V. Y., & Vavilov, S. I. (1999). Comparative investigations of the bolometric properties of thin film structures based on vanadium dioxide and amorphous hydrated silicon. *Proceedings of SPIE 3819* (Vol. 3819, pp. 136-142). Spie. doi:10.1117/12.350896
- Mathur, S., Ruegamer, T., & Grobelsek, I. (2007). Phase-Selective CVD of Vanadium Oxide Nanostructures. *Chemical Vapor Deposition*, 13(1), 42-47. doi:10.1002/cvde.200606578
- Moon, S., Han, Y., Kim, K., Lee, S., & Shin, H. (2005). Enhanced Characteristics of V<sub>0.95</sub>W<sub>0.05</sub>OX-Based Uncooled Microbolometer. *IEEE Sensors, 2005.*, 1137-1140. Ieee. doi:10.1109/ICSENS.2005.1597905
- Moreno, M., Kosarev, A., Torres, A., & Ambrosio, R. (2007). Fabrication and performance comparison of planar and sandwich structures of micro-bolometers with Ge thermo-sensing layer. *Current*, 515, 7607 - 7610. doi:10.1016/j.tsf.2006.11.172
- Motchenbacher, C. D. (1973). *Low Noise Electronic Design*. New York, USA: John Wiley & Sons, Inc.
- Mottin, E., Bain, A., Martin, J. L., Ouvrier-Buffet, J. L., YonN, J. J., Chatard, J. P., & Tissot, J. L. (2002). Uncooled amorphous-silicon technology: high-performance achievement and future trends. *Proceedings of SPIE*, 4721, 56-63. Spie. doi:10.1117/12.478861

- Niklaus, F., Kälvesten, E., & Stemme, G. (2001). Wafer-level membrane transfer bonding of polycrystalline silicon bolometers for use in infrared focal plane arrays. *Journal of Micromechanics and Microengineering*, 11, 509-513.
- Niklaus, F., Vieider, C., & Jakobsen, H. (2007). MEMS-based uncooled infrared bolometer arrays: a review. *Proceedings of SPIE*, 6836, 68360D-68360D-15. Spie. doi:10.1117/12.755128
- Niklaus, Frank, Decharat, A., Jansson, C., & Stemme, Göran. (2008). Performance model for uncooled infrared bolometer arrays and performance predictions of bolometers operating at atmospheric pressure. *Infrared Physics & Technology*, 51(3), 168-177. doi:10.1016/j.infrared.2007.08.001
- Radamson, H. H., Kolahdouz, M., Shayestehaminzadeh, S., Afshar Farniya, A., & Wissmar, S. (2010). Carbon-doped single-crystalline SiGe / Si thermistor with high temperature coefficient of resistance and low noise level. *Applied Physics Letters*, 97(23), 223507. doi:L10-06859R
- Rogalski, a. (2011). Recent progress in infrared detector technologies. *Infrared Physics & Technology*, 54(3), 136-154. Elsevier B.V. doi:10.1016/j.infrared.2010.12.003
- Schimert, T., Brady, J., Fagan, T., Taylor, M., McCardel, W., Gooch, R., Ajmera, S., et al. (2008). Amorphous silicon based large format uncooled FPA microbolometer technology. *Proceedings of SPIE*, 6940, 694023-694023-7. Spie. doi:10.1117/12.784661
- Smith, A., Jones, F. E., & Chasmar, R. P. (1968). *The Detection and Measurement of Infrared Radiation*. Clarendon, Oxford.
- Sood, A. K., Richwine, R. a, Puri, Y. R., DiLello, N., Hoyt, J. L., Akinwande, T. I., Dhar, N., et al. (2010). Development of low dark current SiGe-detector arrays for visible-NIR imaging sensor. *Proc. of SPIE Vol. 7660* (Vol. 7660, pp. 76600L1-7). doi:10.1117/12.852682
- Subrahmanyam, A., Bharat Kumar Redd, Y., & Nagendra, C. L. (2008). Nano-vanadium oxide thin films in mixed phase for microbolometer applications. *Journal of Physics D: Applied Physics*, 41(19), 195108. doi:10.1088/0022-3727/41/19/195108
- Takami, H., Kawatani, K., Kanki, T., & Tanaka, H. (2010). High Temperature-Coefficient of Resistance at Room Temperature in W-Doped VO<sub>2</sub> Thin Films on Al<sub>2</sub>O<sub>3</sub> Substrate and Their Thickness Dependence. *Jpn. J. Appl. Phys.*, 50, 055804.
- Vieider, C., Wissmar, S., Ericsson, P., Halldin, U., Niklaus, Frank, Stemme, G., Kallhammer, J., et al. (2007). Low-cost far infrared bolometer camera for automotive use. *Proceedings of SPIE*, 6542, 65421L-65421L-10. Spie. doi:10.1117/12.721272
- Wang, H., Yi, X., & Chen, S. (2006). Low temperature fabrication of vanadium oxide films for uncooled bolometric detectors. *Infrared Physics & Technology*, 47(3), 273-277. doi:10.1016/j.infrared.2005.04.001
- Wissmar, S., Höglund, L., Andersson, J., Vieider, C., Savage, S., & Ericsson, P. (2006). High signal-to-noise ratio quantum well bolometer materials. *Proceedings of SPIE*, 6401, 64010N-64010N-11. Spie. doi:10.1117/12.689874
- Wissmar, S., Radamson, H., Kolahdouz, M., & Andersson, J. Y. (2008). Ge quantum dots on silicon for terahertz detection. *TERA* (Vol. 6542, pp. 6542-6542).
- Zerov, V. Y., Kulikov, Y. V., Malyarov, V. G., Khrebtov, I. a, Shaganov, I. I., & Shadrin, E. B. (2001). Vanadium oxide films with improved characteristics for ir microbolometric matrices. *Technical Physics Letters*, 27(5), 378-380. doi:10.1134/1.1376757



## **Bolometers**

Edited by Prof. Unil Perera

ISBN 978-953-51-0235-9

Hard cover, 196 pages

**Publisher** InTech

**Published online** 09, March, 2012

**Published in print edition** March, 2012

Infrared Detectors and technologies are very important for a wide range of applications, not only for Military but also for various civilian applications. Comparatively fast bolometers can provide large quantities of low cost devices opening up a new era in infrared technologies. This book deals with various aspects of bolometer developments. It covers bolometer material aspects, different types of bolometers, performance limitations, applications and future trends. The chapters in this book will be useful for senior researchers as well as beginning graduate students.

### **How to reference**

In order to correctly reference this scholarly work, feel free to copy and paste the following:

Henry H. Radamson and M. Kolaoudouz (2012). Group IV Materials for Low Cost and High Performance Bolometers, Bolometers, Prof. Unil Perera (Ed.), ISBN: 978-953-51-0235-9, InTech, Available from: <http://www.intechopen.com/books/bolometers/group-iv-materials-for-low-cost-and-high-performance-bolometers>

**INTECH**  
open science | open minds

### **InTech Europe**

University Campus STeP Ri  
Slavka Krautzeka 83/A  
51000 Rijeka, Croatia  
Phone: +385 (51) 770 447  
Fax: +385 (51) 686 166  
[www.intechopen.com](http://www.intechopen.com)

### **InTech China**

Unit 405, Office Block, Hotel Equatorial Shanghai  
No.65, Yan An Road (West), Shanghai, 200040, China  
中国上海市延安西路65号上海国际贵都大饭店办公楼405单元  
Phone: +86-21-62489820  
Fax: +86-21-62489821

© 2012 The Author(s). Licensee IntechOpen. This is an open access article distributed under the terms of the [Creative Commons Attribution 3.0 License](#), which permits unrestricted use, distribution, and reproduction in any medium, provided the original work is properly cited.

IntechOpen

IntechOpen